Wei *et al. Cancer Cell International* (2025) 25:185
https://doi.org/10.1186/s12935-025-03819-6

Cancer Cell International

RESEARCH Open Access

FAM111B and FANCD2, a dual expression signature, defines a distinct phenotype of pancreatic cancer

Fang Wei[1], Wanying Li[1], Ting Zhou[1], Lijuan Feng[1], Xianglin Yuan[1] and Lihong Zhang[1*]

Abstract

Background Despite various treatment strategies, the incidence and mortality of pancreatic cancer (PC) are among the highest for malignant tumors. Furthermore, there is a lack of effective molecular typing and targeted therapy to treat PC subtypes.

Methods Multiplex immunofluorescence experiments were performed to explore the roles of FAM111B, FANCD2, KRAS and TP53 in human PC tissues. Kaplan-Meier survival curves were generated and a nomogram was prepared for prognostic prediction. Protein correlations were analyzed using human PC tissues and TCGA and GEO data. Pathways analysis, immunoanalysis, and drug susceptibility analysis were performed based on information in the TCGA database.

Results Our results indicate that expression of FAM111B and FANCD2 is correlated in human PC tissues and comprises a dual expression signature with predictive value for the prognosis of PC. Using information in public databases, we confirmed the oncogenic relevance of FAM111B and FANCD2 in PC and identified a positive correlation between FAM111B, FANCD2, TP53 and KRAS.FAM111B and FANCD2 jointly regulate ferroptosis, mitotic nuclear division, and nuclear division pathways. Both proteins were demonstrated to be positively correlated with markers of CD4 + Th2 cells and PD-L1 in the tumor microenvironment. Furthermore, drug sensitivity analysis suggested that patients with high FAM111B or FANCD2 expression were highly sensitive to chemotherapeutic and targeted drugs, indicating that these proteins may serve as predictors of treatment efficacy.

Conclusion Elevated dual expression of FAM111B and FANCD2 is indicative of poor prognosis, alters the immune microenvironment, and exhibits sensitivity to certain therapeutic agents. Consequently, the high FAM111B/FANCD2 expression subtype may represent a novel and distinct phenotype of PC.

Keywords FAM111B, FANCD2, Pancreatic cancer, Prognosis, Immune microenvironment, Molecular subtype

*Correspondence:
Lihong Zhang
lihongzhang@hust.edu.cn
[1]Department of Oncology, Tongji Hospital, Tongji Medical College, Huazhong University of Science and Technology, Wuhan, Hubei 430030, China

© The Author(s) 2025. **Open Access** This article is licensed under a Creative Commons Attribution-NonCommercial-NoDerivatives 4.0 International License, which permits any non-commercial use, sharing, distribution and reproduction in any medium or format, as long as you give appropriate credit to the original author(s) and the source, provide a link to the Creative Commons licence, and indicate if you modified the licensed material. You do not have permission under this licence to share adapted material derived from this article or parts of it. The images or other third party material in this article are included in the article's Creative Commons licence, unless indicated otherwise in a credit line to the material. If material is not included in the article's Creative Commons licence and your intended use is not permitted by statutory regulation or exceeds the permitted use, you will need to obtain permission directly from the copyright holder. To view a copy of this licence, visit http://creativecommons.org/licenses/by-nc-nd/4.0/.

Introduction

Pancreatic cancer (PC) is the tenth most common malignant tumor but the fourth most common cause of mortality [1]. As a result of insidious early symptoms, the majority of patients present with advanced disease at the time of diagnosis [2–4]. Despite various treatments like surgery, radiotherapy, chemotherapy, targeted therapy, and immunotherapy, PC's overall treatment success is still inadequate. Recurrence after radical surgery is around 80% [5, 6], with a five-year survival rate of only 16–21% [7], combined treatments extend median survival to 28–54 months [7–9], and these treatments often cause adverse effects [10–12]. Moreover, there are no effective precision treatment methods based on molecular typing for PC [13]. Therefore, more effective and less toxic treatment strategies are urgently needed for new molecular typing.

FAM111B (family with sequence similarity 111 member B), which plays an important role in carcinogenesis, is also referred to as "Cancer-Associated Nucleoprotein". Studies have demonstrated that FAM111B is overexpressed in breast, lung, ovarian and pancreatic cancers and is associated with the poor patient prognosis [14–17]. FANCD2 (fanconi anemia complementation group D2), a negative regulator of ferroptosis, accelerates the malignant progression of various tumors such as ovarian cancer, lung adenocarcinoma and hepatocellular carcinoma [18–20]. While studies have revealed that FAM111B and FANCD2 each are associated with the poor prognosis of PC [17, 21], there is a lack of research linking FAM111B to FANCD2 in the carcinogenicity of PC.

In this study, we sought to obtain a comprehensive insight into how FAM111B and FANCD2 collaboratively contribute to the carcinogenesis of PC. Multiplex immunofluorescence experiments of tumor tissue microarrays (TMA) confirmed that high expression of both FAM111B and FANCD2 is positively correlated with poor prognosis for PC patients. Bioinformatic analysis verified these findings and identified relevant FAM111B and FANCD2-associated genes and pathways, indicating a novel potential strategy for therapeutic targeting of PC. Our findings suggest that FAM111B and FANCD2 together may function as a novel prognostic factor and biomarker of therapeutic efficacy in PC, which define a distinct targetable phenotype of PC.

Materials and methods

PC tissues

The TMA (HPanA180Su10) was acquired from Shanghai Outdo Biotech Co.Ltd and contained 90 human PC tissue samples with clinicopathologic features and survival information. Due to off-target data in multicolor immunofluorescence experiments, 83 samples were used in the final analysis. The samples included pathological tissue specimens from patients diagnosed with PC and were resected by Whipple's procedure from 2014-01-06 to 2018-12-24 [22]. Among the 83 samples, there were 78 cases of pancreatic ductal adenocarcinoma (PDAC), 2 cases of adeno-squamous carcinoma, 1 case of ampullary adenocarcinoma (pancreaticobiliary type), 1 case of high-grade intraductal papillary mucinous neoplasm with pancreatic ductal adenocarcinoma and 1 case of adenocarcinoma. Clinical information is provided in Supplementary Table 1. The median patient follow-up time was 22 months, with a range of 0-105 months.

Multiplex Immunofluorescence assay

Paraffin-embedded tissue sections were deparaffinized using a solution with fresh xylene and gradient ethanol and then rinsed with sterilized water. Subsequently, the slides were placed in a microwave oven for antigen repair, and a drop of sealing solution was added to cover the sample area. The slides were incubated with antibodies against FAM111B (Novus, NBP1-86645, USA), FANCD2 (Immunoway, YT1675, USA), KRAS (Novus, NBP2-45536, USA), or TP53 (Immunoway, YT3528, USA). Staining and amplification of fluorescent signals were performed using the multiplex fluorescent immunohistochemical staining reagent PANO 7-plex IHC kit, (cat 0004100100, Panovue, Beijing, China). Finally, DAPI working solution was added dropwise, and coverslips were sealed using nail polish. Objective lenses VS200MTL (Olympus Germany) and UPLXAPO20X (Olympus Germany) were used for panoramic scanning of the stained tissue slices. Multidimensional quantitative pathology analysis of multicolor fluorescent images was performed according to five data analysis dimensions (area, cell count, density, ratio and H score) using QuPath v0.3.0 software and constructed with TUMOR, STROMA algorithms. The area referred to the area of fluorescence signal of the proteins; the cell count referred to the number of positive cells (cells positive for specific protein fluorescence expression); the density was the number of positive cells divided by tissue area (mm^2); the ratio was the number of positive cells divided by total number of cells; and the H score referred to the immunofluorescence histochemistry score, using the following formula: [(intensity of 1 + cell positive rate) * 1 + (intensity of 2 + cell positive rate) * 2 + (intensity of 3 + cell positive rate) x 3] * 100. The H score assigns greater weight to cells with higher intensity, thereby incorporating the intensity factor into the calculation of the positive level. This score was derived by multiplying the staining intensity (ranging from 1 to 3) by the percentage of the stained area (ranging from 1 to 100%).

Survival analysis on TMA

Survival analysis of FAM111B and FANCD2 was performed according to the immunohistochemical fluorescence quantification results with the R software "ggsurvplot" package. Kaplan-Meier survival curves were plotted by dividing the samples into high and low groups, using the best cutoff method. The "surv cutpoint" function from the "survminer" package in R software was employed to calculate the cutoff value. The cutoff of FAM111B in the dimensions of area, cell count, density, H score, and ratio were 0.197, 1533, 1424.594, 26.289, and 0.257, respectively; and the cutoff of FANCD2 in the dimensions of area, cell count, density, H score, and ratio were 0.016, 85, 127.242, 2.326, and 0.023, respectively. Expression values less than or equal to the above cutoffs were categorized as the low expression group and those greater than the cutoffs as the high expression group. Multi-group survival analysis for FAM111B and FANCD2 was generated by COX regression using Graphpad 8.0.2.

Nomogram construction

Univariate cox regression analysis was performed by combining FAM111B and FANCD2 with clinical characteristics in PC. According to the results of the analysis, variables indicative of prognosis were automatically enrolled for nomogram construction, which was created by the "rms" R package. The nomogram provided graphical results for these variables in individual patients to predict 1-year, 2-year, and 2.5-year survival, providing a model to guide clinical patient prognosis.

Public database acquisition and analysis

A total of 336 PC tissues and 406 paraneoplastic or normal pancreatic tissues were available in the public database. Clinical information is provided in Supplementary Table 1. The mRNA gene expression data and the clinicopathologic parameters of 179 PC samples and 332 normal pancreatic samples were downloaded from the cancer genome atlas (TCGA: https://portal.gdc.cancer.gov) and Genotype-Tissue Expression (GTEx: https://www.gtexportal.org/home/) databases. The RNA-sequencing data and survival times of 69 PC samples and 61 adjacent pancreatic samples were downloaded from the Gene Expression Omnibus GSE62452 dataset; RNA-sequencing data were also accessed from 118 PC samples and 13 adjacent pancreatic samples in the GSE62165 dataset (https://www.ncbi.nlm.nih.gov/geo/). The LOGpc online tool (https://bioinfo.henu.edu.cn/) was *u*sed for the screening of PC samples in TCGA and GEO datasets, based on survival curves with gene expression median value grouping. The FAM111B or FANCD2 expression level was categorized into high and low groups based on the median expression level.

Transcriptomic analysis

To clarify the prognostic value of FAM111B or FANCD2 expression in PC, we performed Kaplan-Meier survival analysis using an online platform (https://www.bioinformatics.com.cn) for data analysis and visualization. The "timeROC" package of R software was used to generate receiver operating characteristic (ROC) curves to assess the prognostic validity of the model. The somatic mutation oncoplot was generated using the "maftools" package in R software for exploring genes mutations in PC patients. Gene expression plots in patients with TP53 mutations or KRAS mutations were generated using the online analysis tool TIMER 2.0 (http://timer.cistrome.org/).

Ferroptosis pathway analysis

To explore the relationship between FAM111B and the ferroptosis pathway, 24 ferroptosis-related geneswere analyzed [23]. A heatmap was generated using the R software "ggplot2" and "pheatmap" packages. Ferroptosis-related genes were analyzed for consistency using the R package "Consensus Cluster Plus". The number of clusters was 2, and the genes were categorized into high and low expression groups for survival analysis. Moreover, analysis of the correlation between FAM111B and the pathway scores was performed using the R software "GSVA" package, applying the ssGSEA algorithm.

Enrichment analysis of downstream genes

Volcano maps were generated by the "enhanced volcano" R package to display differentially expressed genes. To explore the signaling pathways involved with FAM111B and FANCD2, sets of genes were collected that were elevated in both the FAM111B and FANCD2 high expression groups for GO (gene-ontology) and KEGG (kyoto encyclopedia of genes and genomes) enrichment analysis with the R software "Cluster Profiler" package.

Immunoanalysis

To explore the role of FAM111B in the PC immune microenvironment, we applied the immunedeconv R package XCELL algorithm for immune scoring according to TCGA database. The ggplot2 and pheatmap R packages were further used to generate an immune cell distributiongraph, immune cell scoring heatmaps and percentage abundance heatmaps of immune cell infiltration. The mRNA expression levels of the immune checkpoint-related genes SIGLEC15, TIGIT, PD-L1, HAVCR2, PDCD1, CTLA4, LAG3 and PDCD1LG2 were also extracted for expression difference analysis and immunotherapy evaluation.

Drug susceptibility analysis

The sensitivity to chemotherapy and targeted therapy were predicted for all PC samples through the pharmacogenomics database Genomics of Drug Sensitivity in Cancer (GDSC: https://www.cancerrxgene.org/) using the "pRRophetic" R package. Each samples' half-maximal inhibitory concentration (IC50) was estimated by ridge regression.

Statistical analysis

Statistical analysis was performed by the Wilcoxon's rank sum test for two groups and Kruskal-Wallis one-way ANOVA for comparing differences among three or more groups using R software v4.0.3 (R Foundation for Statistical Computing, Vienna, Austria). Log-rank statistical tests were applied to compare survival curves between two groups. Cox regression analysis was utilized for evaluating multiple survival curves. Gene correlation analysis was performed using the Spearman algorithm. Results were considered statistically significant when the P-value was less than 0.05. The asterisks (*) stands for the significance of the p-value, $^{*}P<0.05$, $^{**}P<0.01$,$^{***}P<0.001$.

Results

FAM111B and FANCD2 are over expressed in PC and predict poor patient prognosis

To evaluate whether FAM111B and FANCD2 may serve as biomarkers for PC, we conducted multiplex immunofluorescence experiments, based on five data analysis dimensions (area, cell count, density, H score, and ratio), on 83 patients with PC. The co-expression immunofluorescence images for FAM111B and FANCD2 are presented in Fig. 1A. According to the results, FAM111B and FANCD2 were positively correlated in each of the five dimensions (Fig. 1B-F, all $P<0.05$), and this conclusion remained consistent in the subgroup analysis of 78 PDAC cases (Supplementary Fig. 1A-E, all $P<0.05$). In patients with a survival duration of less than 45 months, OS was significantly reduced in those exhibiting high expression levels of FAM111B and FANCD2 compared to those with low expression levels (Fig. 2A-J, all $P<0.05$). This trend was similarly observed in a cohort of 78 PDAC cases (Supplementary Fig. 1F-O, all $P<0.05$). The TMA analyzed includes patients who underwent adjuvant therapy, which was found to influence OS (Supplementary Fig. 2A; Supplementary Fig. 2B, $P<0.05$). Furthermore, among patients who underwent surgical treatment without subsequent adjuvant therapy, elevated expression of FAM111B and FANCD2 was also correlated with decreased OS (Supplementary Fig. 3A-J, all $P<0.05$). Significantly, combining survival analyses demonstrated that patients with double high expression of FAM111B and FANCD2 had the shortest OS, while patients with double low expression had the longest OS (Fig. 2K-O, all $P<0.05$). These results suggest that FAM111B and FANCD2 both contribute to the poor prognosis of PC patients.

For additional prognostic evidence, we conducted univariate COX regression analysis according to clinical data from 54 patients. FAM111B, FANCD2, grade (G3 vs. G2), tumor size, CA125 and CA199 were found to independently predict the prognosis of PC (Fig. 3A, all $P<0.05$). A calculated hazard ratio exceeding 1 was considered an adverse prognostic factor and was therefore incorporated into the nomogram building using FAM111B (HR = 3.098), FANCD2 (HR = 2.652), and tumor size (HR = 1.177) factors. To develop a clinically applicable method for predicting the probability of patient survival, we constructed a predictive model for 1-year, 2-year and 2.5-year survival (Fig. 3B). The total points were combined for each variable on a scale of 0-240, with higher totals indicating worse patient prognosis. To assess the validity of nomogram plot, we further built a calibration curve, in which the dashed line indicates a reference for determining how closely the predicted probability matches the observed probability. The calibration curves indicate an estimation of 1-year, 2-year and 2.5-year OS for the nomogram plot with favorable performance (Fig. 3C).

To further extend our findings, we utilized publicly available databases to confirm that high expression of FAM111B and FANCD2 is indicative of an unfavorable prognosis in PC patients. FAM111B and FANCD2 expression was verified to be significantly overexpressed in 366 PC patients compared to paracancerous or normal tissues based on TCGA and GEO datasets (all $P<0.0001$) (Fig. 4A-F). Furthermore, FAM111B was found to be positively correlated with FANCD2 among 37 of 39 tumors in the TCGA database (Fig. 4G), including PC in TCGA($R=0.567$, $P<0.001$), as well as in GSE62452 ($R=0.748$, $P<0.001$) and GSE62165 ($R=0.603$, $P<0.001$) datasets from GEO database (Fig. 4H-J). Kaplan-Meier survival plots demonstrated that high FAM111B and FANCD2 expression was associated with shorter OS (all $P<0.05$) (Fig. 5A-D). Additionally, in timeROC analysis, the AUCs of three-year survival from the TCGA and GEO datasets were 0.74 and 0.81for FAM111B; and 0.72 and 0.84for FANCD2, respectively (Fig. 5E-H), thus verifying the predictive potential of FAM111B and FANCD2 expression. Spearman correlation analysis further demonstrated that FAM111B and FANCD2 were positively associated with the stemness index based on mRNA expression (mRNAsi [24] ($R=0.18$, $P=0.013$; $R=0.21$, $P=0.005$) (Fig. 5I, J). Moreover, the Kruskal-Wallis test confirmed that the expression of FAM111B and FANCD2 were significantly correlated with pathological grade (both $P<0.0001$) (Fig. 5K, L). These results suggest that

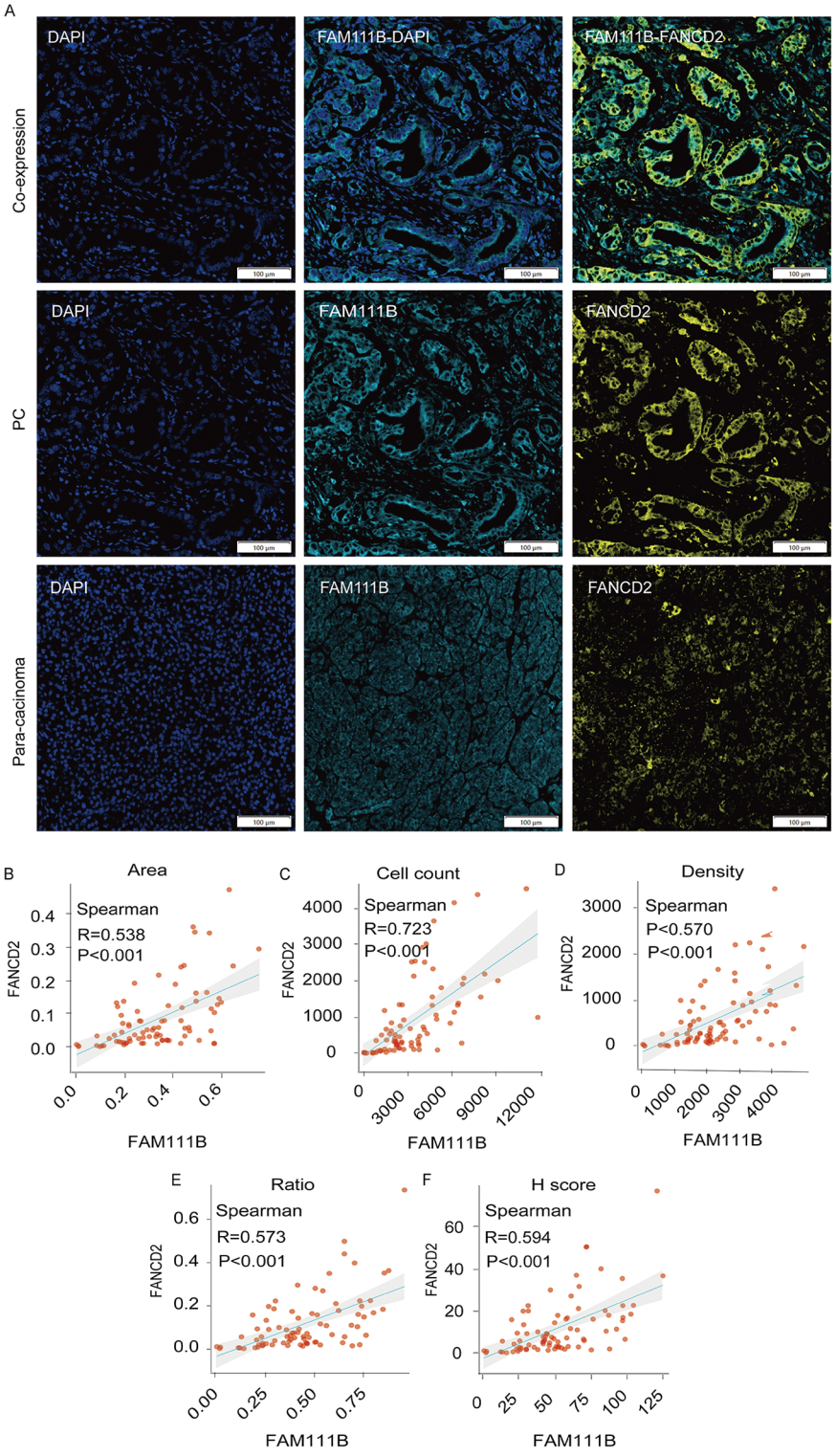

Fig. 1 FAM111B expression positively correlates with FANCD2 expression in human PC tissues. **A** Representative images of FAM111B and FANCD2 in PC and para-carcinoma. **B-F** FAM111B positively correlates with FANCD2 in five dimensions: area, cell count, density, H score, and ratio

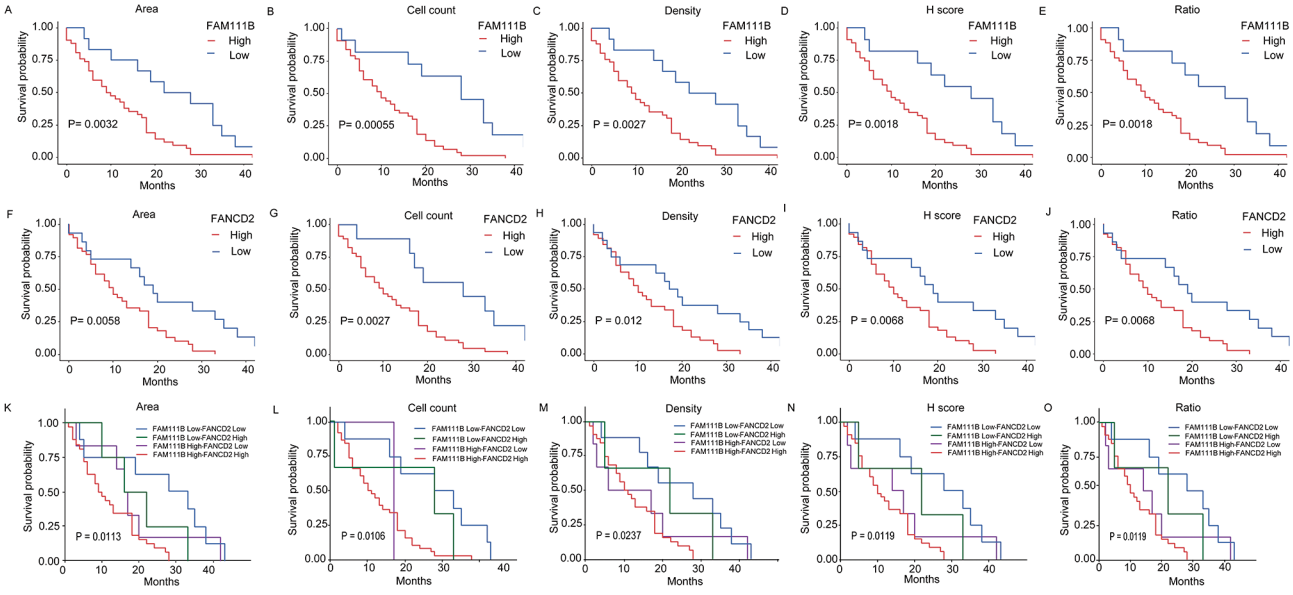

Fig. 2 Survival curves for patients expressing high or low FAM111B and FANCD2. **A-E** Survival curves for FAM111B in five dimensions. **F-J** Survival curves for FANCD2 in five dimensions. **K-O** Multiplex survival curves based on FAM111B and FANCD2

FAM111B and FANCD2 are associated with malignant pathological features and poor prognosis of PC.

FAM111B and FANCD2 are correlated with TP53 and KRAS in PC

To explore a potential correlation of FAM111B and FANCD2 with the mutation status of PC, we performed mutation analysis of samples from the TCGA database. KRAS and TP53 mutations occurred in 77% and 64% in PC patients, respectively (Fig. 6A). Moreover, FAM111B and FANCD2 were highly expressed in both KRAS- and TP53-mutated patients (Fig. 6B-E, all $P<0.05$). Correlation analysis demonstrated that FANCD2 and FAM111B each were positively associated with TP53 and KRAS (all $P<0.001$, Fig. 6F-I). Co-expression immunofluorescence assays confirmed these results (Figs. 7 and 8). Furthermore, the positive correlation of FANCD2 and FAM111B with TP53 and KRAS was evidenced in the analysis of each of the five parameter dimensions: area, cell count, density, H score, and ratio (Figs. 7 and 8 and B-K, both $P<0.05$). The same conclusion was drawn in the subgroup analysis of 78 PDAC cases (Supplementary Fig. 4A-T, all $P<0.05$). These results are consistent with the possibility that FAM111B and FANCD2 might play roles in TP53 and KRAS mutant PC.

FAM111B and FANCD2 are collaboratively involved in signaling pathways in PC

To explore the biological processes and pathways associated with FAM111B and FANCD2 expression, we performed differential expression analysis from TCGA database. Volcano plots suggested that 39 genes were up-regulated in both FAM111B and FANCD2 high expression groups (Fig. 9A-C). GO enrichment analysis demonstrated that these genes were enriched in mitotic nuclear division, nuclear division, and organelle fission pathways (Fig. 9D). Furthermore, KEGG enrichment analysis demonstrated that FAM111B and FANCD2 were jointly involved in a variety of regulatory pathways, including the ECM-receptor interaction, focal adhesion and PI3K-Akt signaling pathway (Fig. 9E). Notably, the expression of FAM111B was positively correlated with the majority of ferroptosis pathway molecules (Fig. 9F). According to consensus clustering analysis, when the clustering variable (k) was set to 2, 179 PC patients could be divided into two clusters (Fig. 9G), with the ferroptosis pathway molecules expressed significantly higher in cluster 1 than 2 (Fig. 9H). Kaplan-Meier survival curves revealed shorter OS in cluster 1($P=0.0016$) compared to cluster 2 (Fig. 9I). Correlation analysis further verified that FAM111B expression was associated with the ferroptosis regulatory pathway and the cellular response to hypoxia pathway, and was inversely associated with the oxidative phosphorylation and fatty acid degradation pathways in PC (Fig. 9J-M, all $P<0.05$).

FAM111B and FANCD2 expression is associated with a favorable tumor immune microenvironment

The tumor microenvironment, including immune cells, stromal cells, and cytokines, plays an important role in tumor development, metastasis, recurrence and treatment response [25]. From the TCGA database, we analyzed the correlation between the expression of FAM111B or FANCD2 and the tumor microenvironment

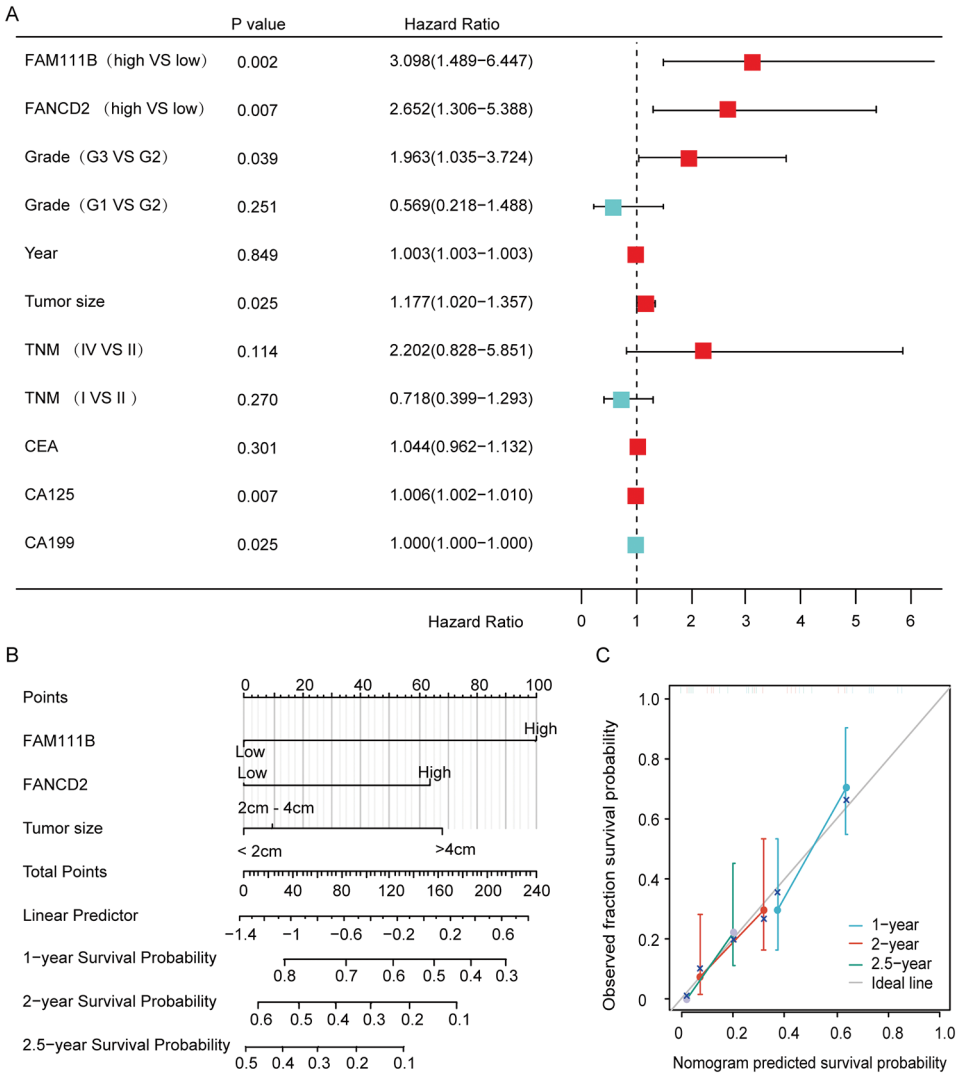

Fig. 3 Clinical nomogram based on FAM111B and FANCD2 expression. **A** Univariate regression analysis between FAM111B, FANCD2, and clinical factors. **B** Prognosis predictive model. **C** Calibration curve for overall survival according to the nomogram model

using the XCEL algorithm. The results suggest that the level of immune cell infiltration is different in the high and low FAM111B or FANCD2 expression groups (Fig. 10A-B). Specifically, CD4 + Th2 cells were positively correlated, while hematopoietic stem cells and stromal scores were negatively correlated with FAM111B and FANCD2 expression (Fig. 10C-E; F-H, all $P < 0.05$). Notably, the immune checkpoint molecule PD-L1 was highly expressed in the FAM111B and FANCD2 high expression groups (Fig. 10I-J both $P < 0.05$). Finally, correlation analysis demonstrated that both FAM111B and FANCD2 were positively correlated with PD-L1, based on the TCGA, GSE62452 and GSE62165 datasets (Fig. 10K-M; N-P, all $P < 0.05$). Therefore, these results suggest that expression of FAM111B and FANCD2 is associated with immune cell infiltration and upregulation of PD-L1, which could potentially be indicative of the improved therapeutic efficacy of PD-1 or PD-L1 immune checkpoint inhibitors in PC.

FAM111B and FANCD2 improve therapeutic responsiveness in PC

To predict the association of FAM111B and FANCD2 expression with responsiveness to chemotherapy and molecular targeted therapy, we used the half-maximal inhibitory concentration (IC50) in the GDSC database to estimate the chemotherapy response among 179 PC patients. The results demonstrate that patients with higher expression of FAM111B or FANCD2 required lower IC50 for gemcitabine, 5-fluorouracil, paclitaxel, gefitinib, sunitinib and sorafenib (all $P < 0.05$) (Fig. 11A-F). These results suggest that patients with high FAM111B and FANCD2 expression may be more

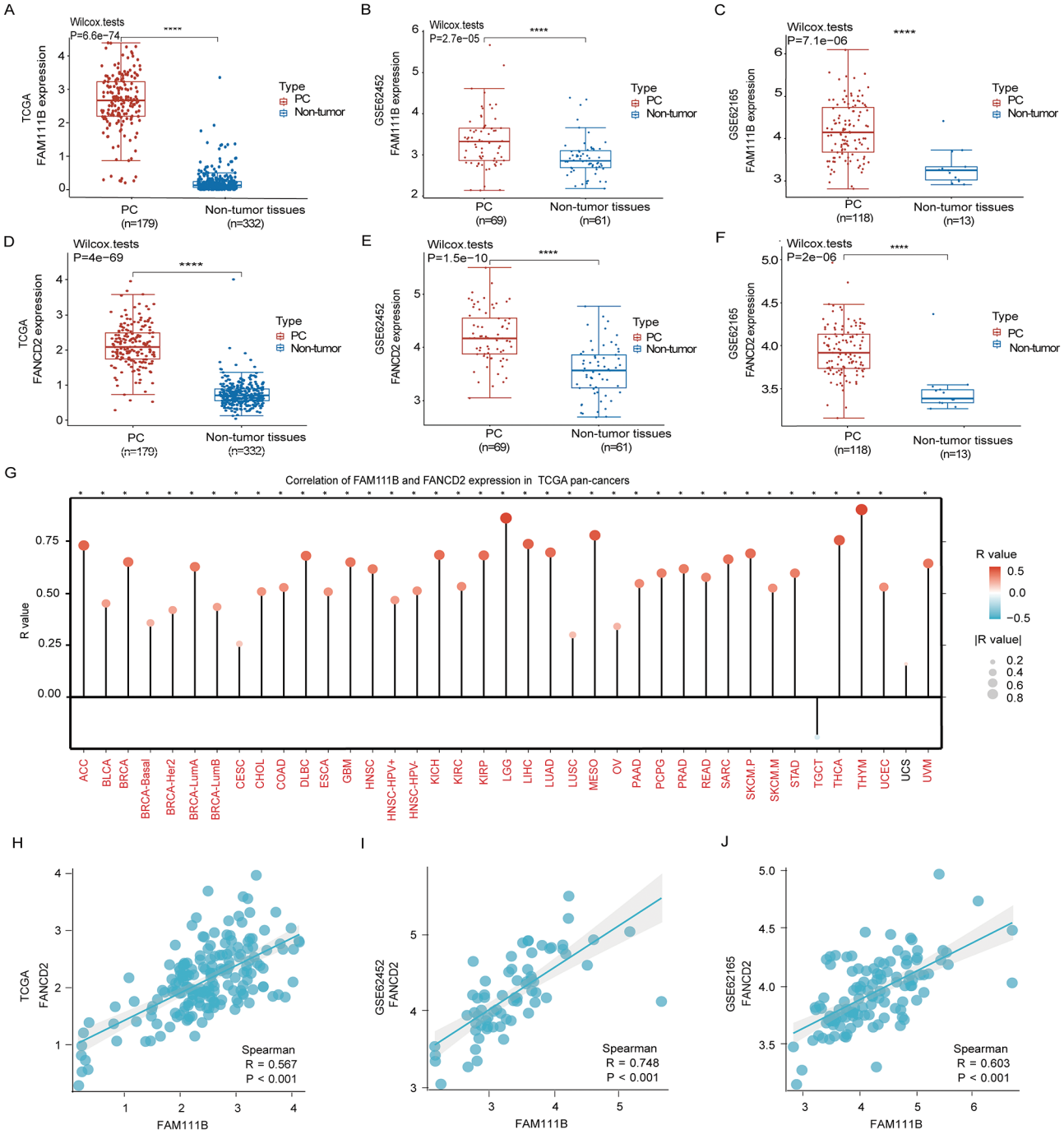

Fig. 4 Analysis of the correlation between FAM111B or FANCD2 in samples from the TCGA and GEO databases. **A-F** Expression distribution plots for FAM111B and FANCD2 in TCGA, GSE62452, and GSE62165. **G** Correlation analysis of FAM111B and FANCD2 expression in 39 pan-cancers. **H-J** Association between FAM111B and FANCD2 in TCGA, GSE62452, and GSE62165

sensitive to chemotherapy, indicating that these proteins may serve as novel predictors of therapeutic efficacy.

Discussion

Current research suggests that FAM111B and FANCD2 may have oncogenic roles in various cancers, including ovarian, liver, lung, and breast cancers [26, 27]. Our study is the first to link FAM111B to FANCD2, showing that the two proteins jointly play a significant role in the malignant process of PC. We confirmed the correlation between FAM111B and FANCD2 as a dual signature that predicts patient prognosis. Furthermore, our bioinformatics analysis suggests that FAM111B and FANCD2 regulate the ferroptosis pathway and alter the immune

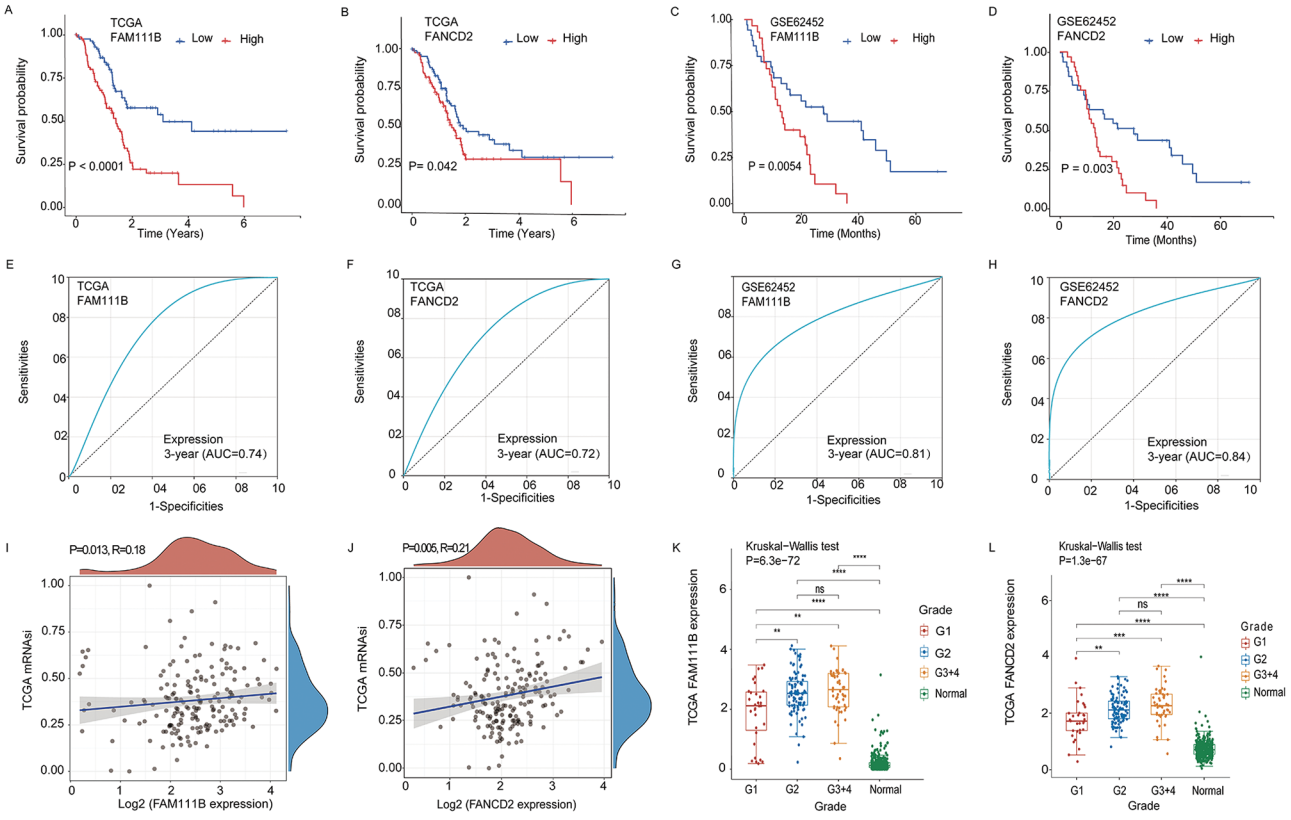

Fig. 5 Analysis of FAM111B or FANCD2 expression and patient prognosis according to TCGA and GEO databases. **A-D** Kaplan Meier survival curves according to FAM111B and FANCD2 expression for patients in the TCGA and GSE62452 databases. **E-H** TimeROC curves according to FAM111B and FANCD2 expression for patients in the TCGA and GSE62452 databases. **I-J** Association between FAM111B or FANCD2 expression and mRNAsi in TCGA. **K-L** Association between FAM111B or FANCD2 expression and the pathological grade in TCGA

microenvironment. Additionally, high expression of these proteins may increase the sensitivity of chemotherapy and targeted drugs, potentially serving as predictors of treatment effectiveness.

Our finding that FAM111B and FANCD2 expression is associated with ferroptosis is consistent with the results of previous studies. Ferroptosisis a type of cell death caused by an excess of ferric ions leading to oxidative stress and lipid peroxidation, ultimately destroying the cell membrane [28, 29]. FANCD2, an inhibitor of ferroptosis, suppresses lipid peroxidation and reduces ferric ion accumulation, contributing to the enhanced resistance of tumor cells to oxidative stress [28, 30]. Our study demonstrates for the first time that FAM111B is positively correlated with FANCD2. Elevated levels of reactive oxygen species generated during ferroptosis have been demonstrated to trigger the formation of covalent DNA-protein cross-links within the nucleus, whereas the FAM111 protein family facilitates hydrolysis, thereby preserving DNA integrity [31]. Our results indicate that FAM111B expression is also associated with cellular oxidative response, raising the possibility that FAM111B and FANCD2 may collaboratively participate in the regulation of ferroptosis through the modulation of intracellular ferric ions or lipid peroxidation.

Our observations indicate that the upregulation of FAM111B and FANCD2 is associated with mutations in TP53 and KRAS in PC. Previous studies have demonstrated that the inhibition of FAM111B or FANCD2 leads to increased arrest in the G0/G1 and G2/M phases of the cell cycle in cancer cells, thereby impacting TP53 and KRAS pathways [32–34]. Specifically, in KRAS-mutant lung adenocarcinoma (LUAD) cells, the silencing of FAM111B impedes the G0/G1 phase transition and cell proliferation [14]. In hepatocellular carcinoma (HCC) and LUAD cells, the silencing of FAM111B results in increased arrest in the G0/G1 or G2/M phases, respectively, and which activated the TP53 pathway [32, 33]. Additionally, in osteosarcoma, the inhibition of FANCD2 promotes TP53 phosphorylation and G1 phase arrest [34]. These findings suggest that FAM111B and FANCD2 may facilitate cancer cell proliferation by promoting cell cycle transitions through the activation of the TP53 pathway, particularly in cancers with KRAS mutations.

Notably, mutations in KRAS and TP53 are observed in 77% and 64% of cases, respectively. This study proposes that linking FAM111B and FANCD2 with KRAS

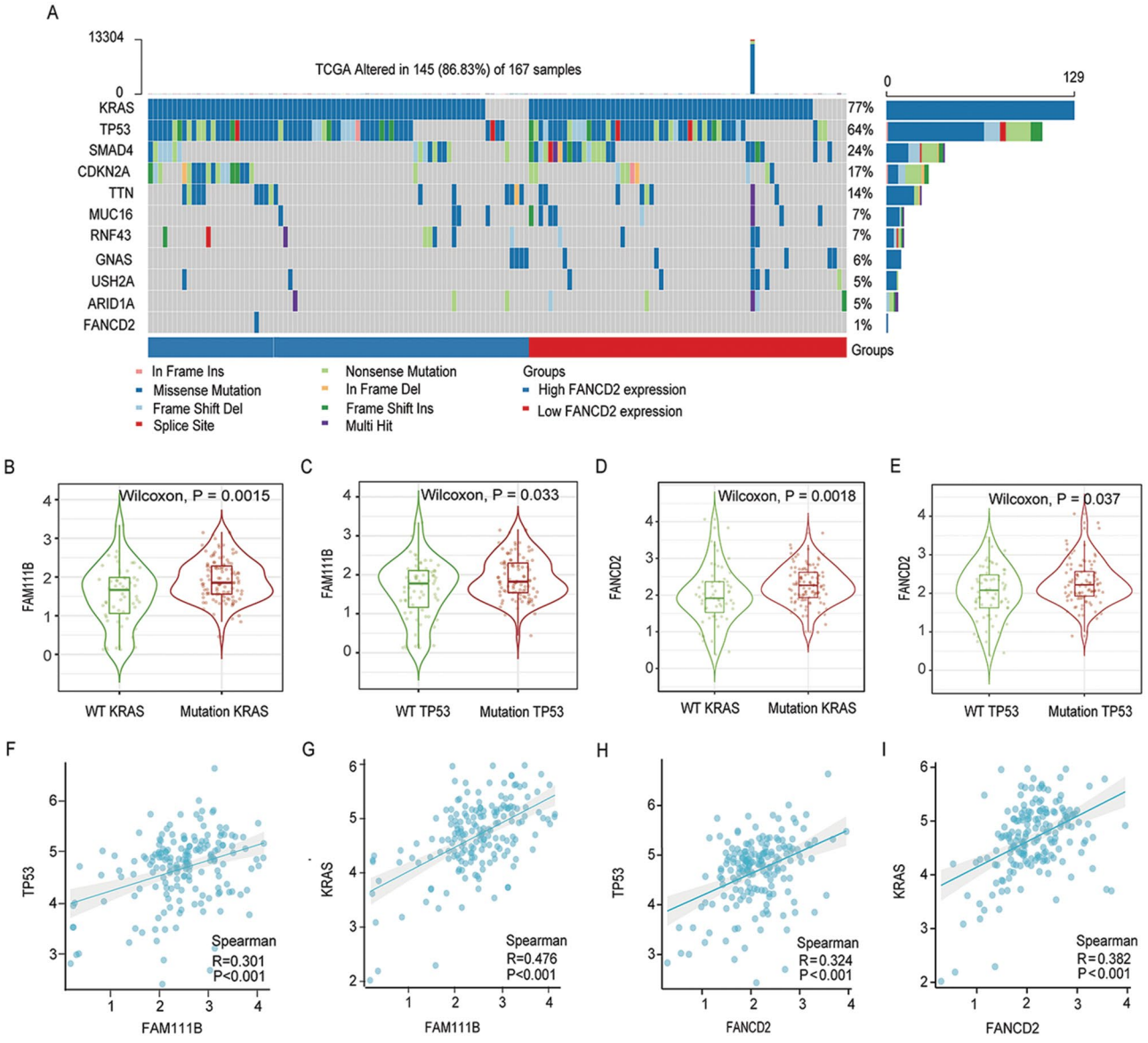

Fig. 6 Mutation analysis of FANCD2 and FAM111B in PC based on TCGA database. **A** Mutational analysis of FANCD2 in PC. **B-E** Expression of FANCD2 or FAM111B in PC patients with TP53 and KRAS mutants. **F** Association between FANCD2 and TP53. **G** Association between FANCD2 and KRAS. **H** Association between FAM111B and TP53. **I** Association between FAM111B and KRAS

and TP53 mutations may present viable treatment options, suggesting that therapies targeting FAM111B and FANCD2, in combination with KRAS inhibitors or TP53 antagonists, could offer novel insights into molecularly targeted therapy for PC. Furthermore, the observed positive correlation between FAM111B/FANCD2 overexpression and PDL-1 expression indicates the potential efficacy of PD-1 and PDL-1 inhibitors. Additionally, chemotherapeutic agents such as gemcitabine and 5-fluorouracil, which may demonstrate increased sensitivity in this subtype, warrant further investigation. Over the next five years, it is anticipated that the dual overexpression of FAM111B and FANCD2 in PC will be employed for preliminary prognosis prediction and to inform the selection of targeted treatment strategies.

Importantly, we demonstrated that FAM111B and FANCD2 may have predictive value for the prognosis of patients with a survival of less than 45 months. We selected 45 months as a threshold because clinical studies on adjuvant chemotherapy after surgery have revealed that the median survival time in the GX group (gemcitabine and capecitabine), the MFOLFIRINOX group (oxaliplatin, irinotecan, and leucovorin), and the AG group (gemcitabine and albumin-bound paclitaxel) compared to the G group (gemcitabine monotherapy), were 28 months VS. 25 months [7], 54 months VS. 35 months

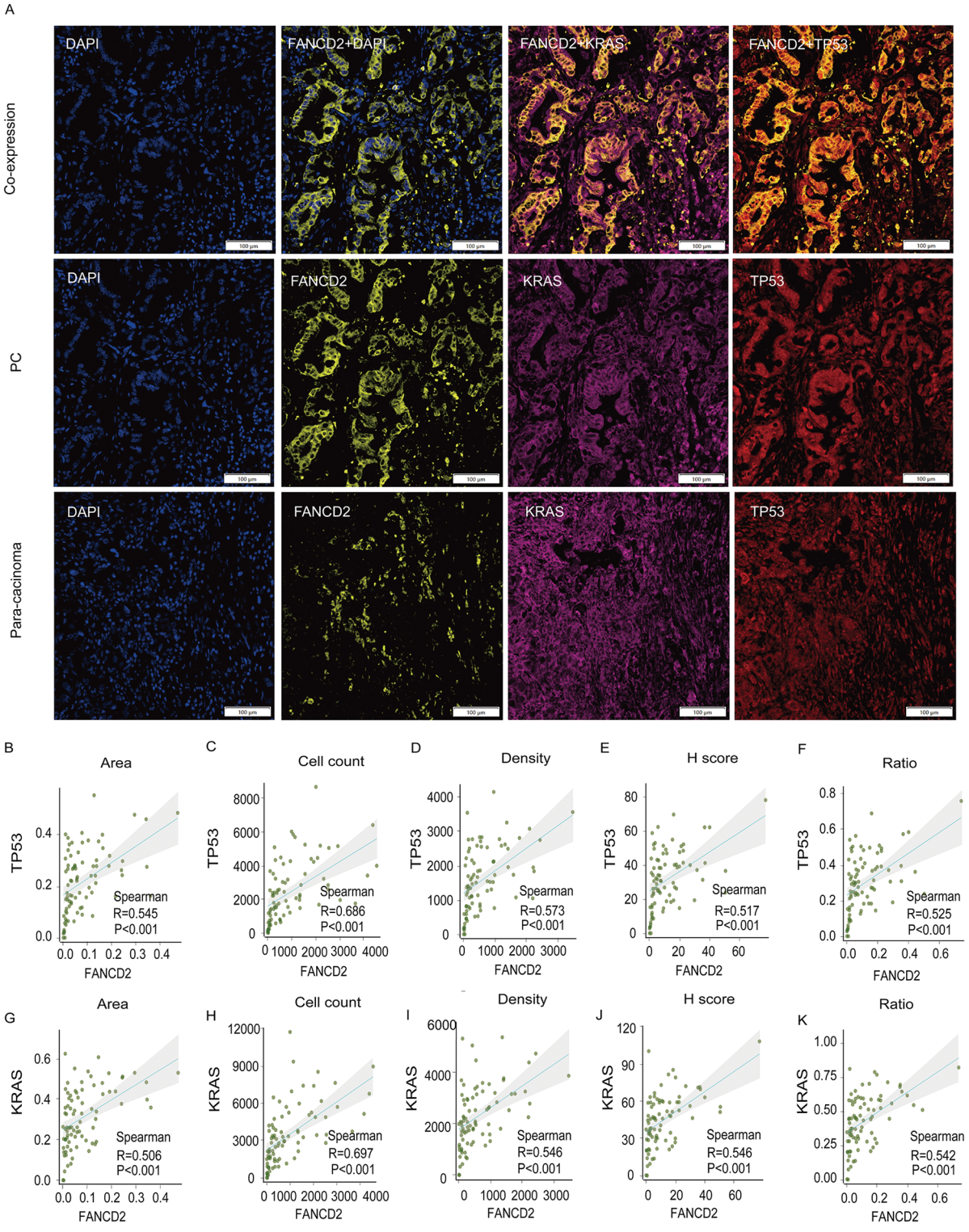

Fig. 7 FANCD2 positively correlates with TP53 and KRAS in human PC tissues. **A** Representative images of FANCD2, TP53 and KRAS are shown for PC and para-carcinoma tissues. **B-K** FANCD2 positively correlates with TP53 and KRAS in five dimensions

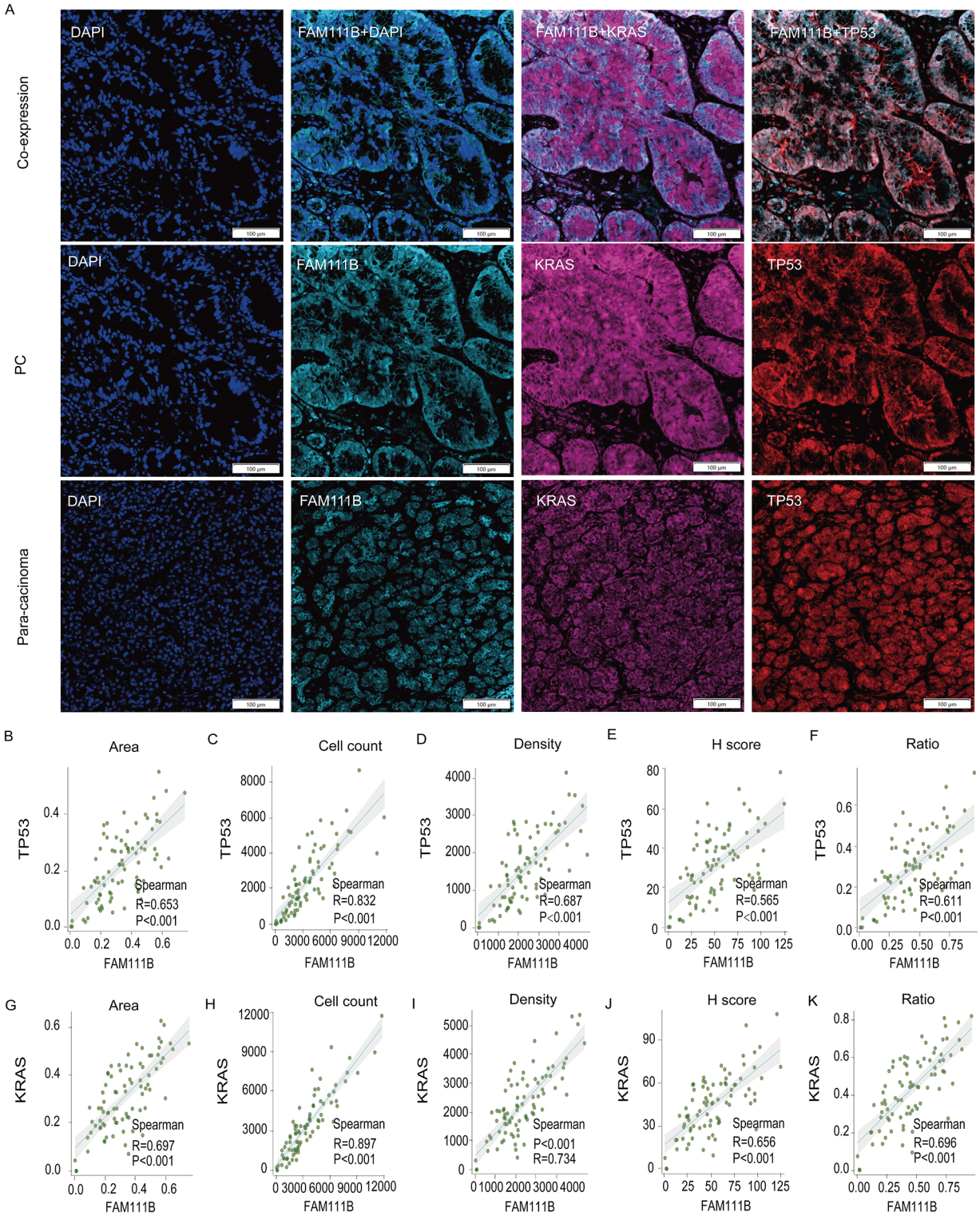

Fig. 8 FAM111B positively correlates with TP53 and KRAS in human PC tissues. **A** Representative images of FAM111B, TP53 and KRAS are shown for PC and para-carcinoma tissues. **B-K** FAM111B positively correlates with TP53 and KRAS in five dimensions

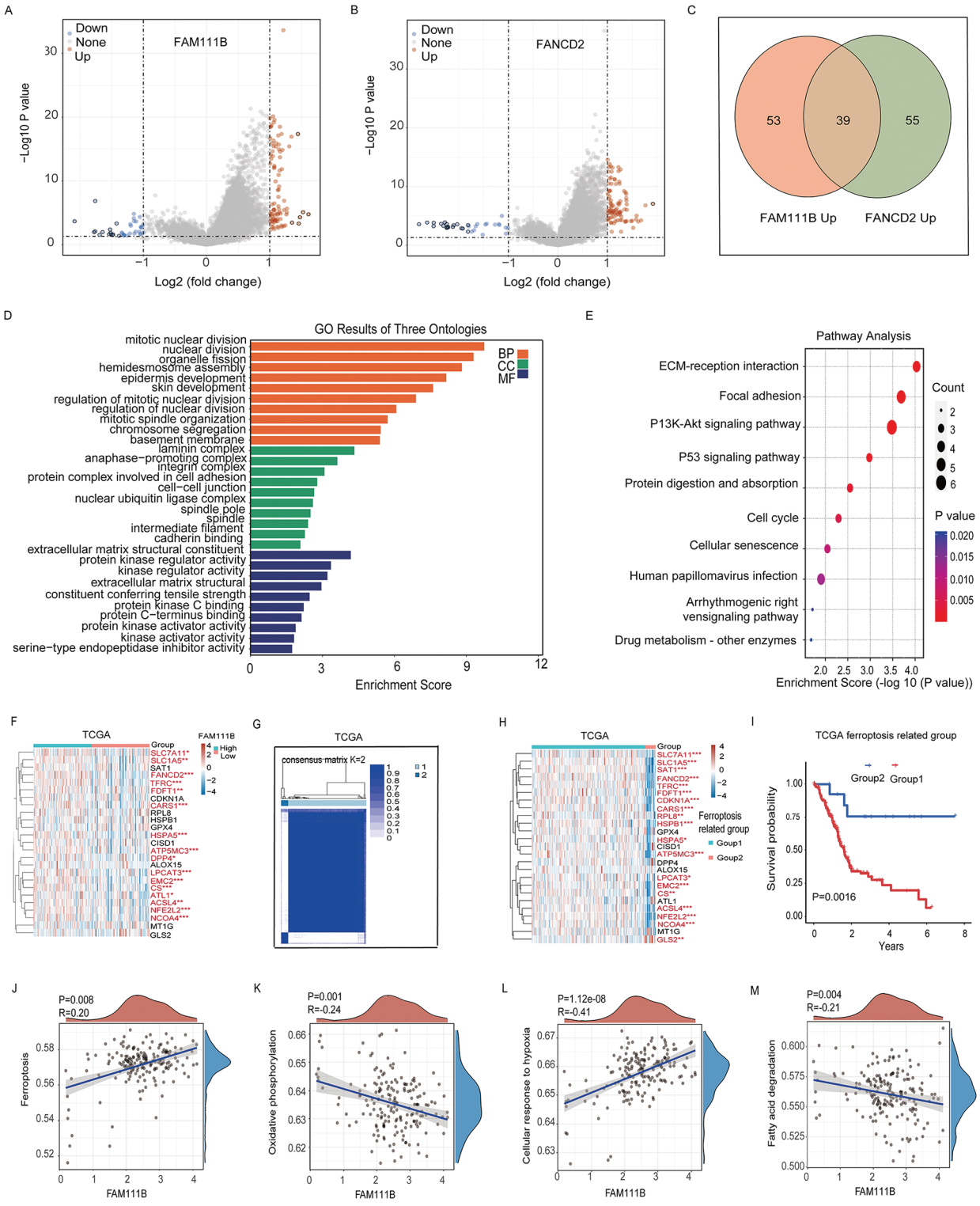

Fig. 9 Signaling pathways associated with FAM111B and FANCD2 expression in PC. **A** Volcano graph of FAM111B expression in PC. **B** Volcano graph of FANCD2 expression in PC. **C** Venn diagram of upregulated genes in FAM111B and FANCD2 high expression patients. **D** GO enrichment analysis of genes upregulated in FAM111B- and FANCD2-high patients. **E** KEGG enrichment analysis of genes upregulated in FAM111B- and FANCD2-high patients. **F** Heatmap of ferroptosis genes among PC patients with low and high FAM111B expression. **G** Consensus clustering matrix (k = 2) of associated genes. **H**: Heatmap of groups with low (Group 1) and high (Group 2) expression of ferroptosis genes. **I** Kaplan-Meier survival analysis for Groups 1 and 2. **J-M** Association of FAM111B expression with the Ferroptosis pathway, Oxidative phosphorylation pathway, Cellular response to hypoxia pathway, and Fatty acid degradation pathway

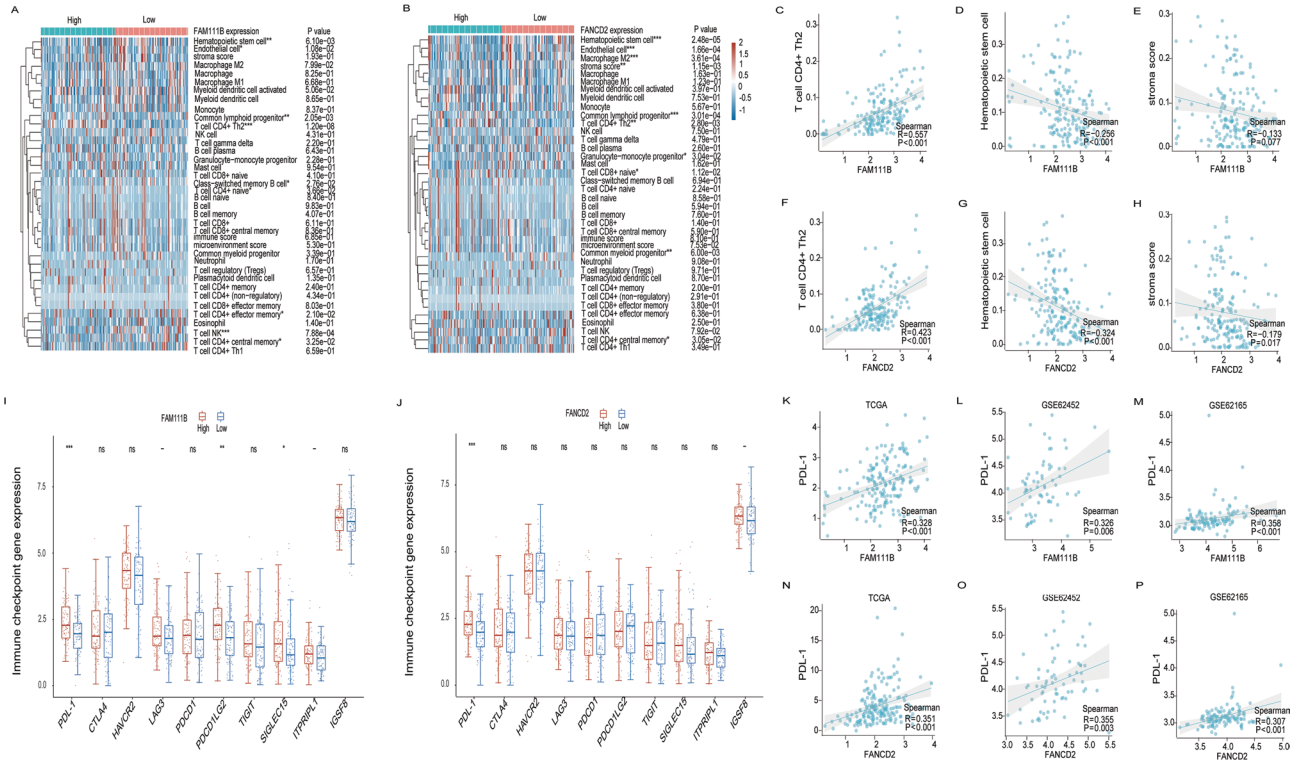

Fig. 10 Evaluation of the association of FAM111B and FANCD2 with the tumor immune microenvironment. **A-B** Heat maps of immune cell marker genes in samples with low or high FAM111B and FANCD2 expression. **C-E** Correlation between FAM111B expression and the expression of CD4 + Th2 cell genes, hematopoietic stem cell genes and stroma scores. **F-H** Correlation between FANCD2 expression and the expression of CD4 + Th2 cell genes, hematopoietic stem cell genes and stroma scores. **I-J** Scatter plots of immune checkpoint gene expression in samples with low or high FAM111B and FANCD2 expression. **K-M** Correlation between FAM111B and PD-L1 expression in TCGA, GSE62452 and GSE62165 datasets. **N-P** Correlation between FANCD2 and PD-L1 expression in TCGA, GSE62452 and GSE62165 datasets

[9], and 42 months VS. 37 months [8], respectively. Therefore, 45 months reflects a median survival time of the majority of PC patients after surgery. Additionally, our survival prediction model also showed that the prediction power of FAM111B/FANCD2 is optimal within two and a half years, which is consistent with more significant prediction value for patients with shorter survival.

We also demonstrated that FAM111B and FANCD2 play a synergistic role in the regulation of the PC immune microenvironment, given that their expression is positively correlated with the immune checkpoint protein PD-L1. Our previous research also revealed a positive correlation between FAM111B and PD-L1 in ovarian cancer [16]. Ferroptosis-inducing agents and immune checkpoint blockers have been shown to have a synergistic therapeutic effect in a GBM mouse model [35] and to effectively inhibit the proliferation of HCC cells [36]. Therefore, we speculate that the combination of ferroptosis inducers and immunotherapy may provide an effective strategy for patients with high FAM111B and FANCD2 expression. Our results suggest that the FAM111B/FANCD2 high expression group was more sensitive than the FAM111B/FANCD2 low expression group to gemcitabine, 5-fluorouracil, paclitaxel, gefitinib, sunitinib and sorafenib. Consistently, another study demonstrated that PC patients with high FANCD2 expression are more sensitive to 5-fluorouracil and sorafenib [21]. Sorafenib induces cells to trigger ferroptosis by inhibiting the P62-Keap1-Nrf2 signaling pathway [37], which may partially explain the latter results. Given that gefitinib is an EGFR inhibitor, we postulate that patients with high FAM111B expression may have elevated EGFR expression levels, rendering them responsive to EGFR inhibitors. This hypothesis is further supported by the positive correlation between FAM111B and EGFR identified in our team's previous study on ovarian cancer [16].

This study is subject to two primary limitations. First, technical constraints limited our ability to perform immunofluorescence exclusively on TMA samples, thereby precluding genotyping. Furthermore, the absence of specific mutation site data for KRAS and TP53 in the TCGA database impeded additional genotyping analyses. Second, the conclusions are based solely on results from TMA and bioinformatics analyses. In future research, we intend to substantiate our findings through a combination of in vitro and in vivo experiments.

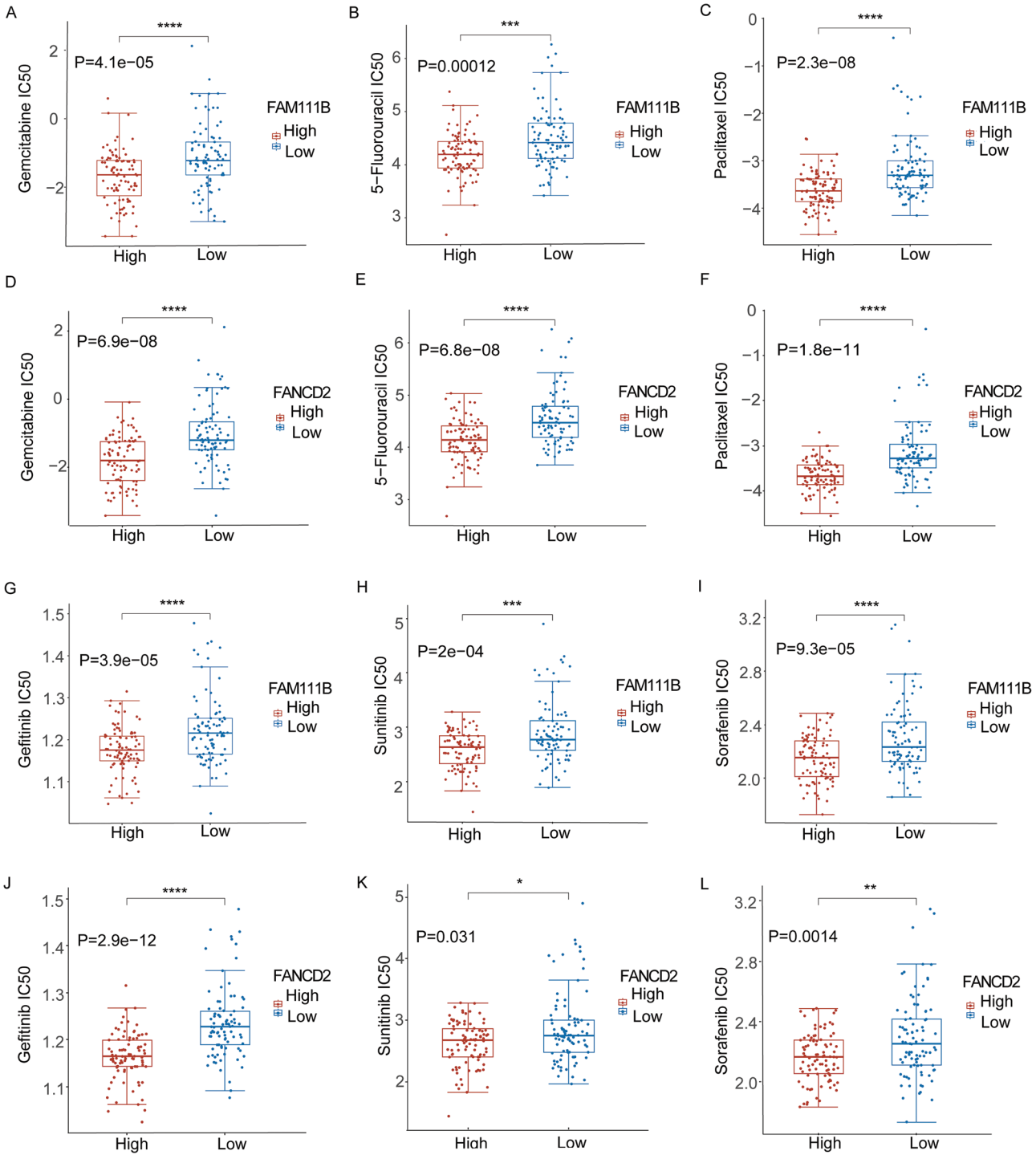

Fig. 11 Efficacy analysis of therapeutic drugs for FAM111B and FANCD2 in PC. The IC50 value of FAM111B in samples from patients treated with **A** Gemcitabine, **B** 5-Fluorouracil, **C** Paclitaxel. The IC50 value of FANCD2 in samples from patients treated with **D** Gemcitabine, **E** 5-Fluorouracil, **F** Paclitaxel. The IC50 value of FAM111B in samples from patients treated with **G** Gefitinib, **H** Sunitinib, **I** Sorafenib. The IC50 value of FANCD2 in samples from patients treated with **J** Gefitinib, **K** Sunitinib, **L** Sorafenib

Conclusion

In conclusion, PC lacks effective molecular typing and precision treatment strategies for molecular subtypes. Consequently, the greatest contribution of our research is perhaps the creation of a new molecular typing method for PC, which could be a simple and effective prognostic approach. Double high expression of FAM111B and FANCD2 defines distinct biological characteristics,

including poorer prognosis, heightened aggressiveness, altered immune microenvironment, and enhanced responsiveness to specific drugs. Our research provides insights into a novel molecular subtyping strategy, as well as a potential precision treatment approach for PC.

Abbreviations

PC	Pancreatic cancer
GNP	Gemcitabine and nab-paclitaxel
FOLFIRINOX	5-fluorouracil, leucovorin, irinotecan, and oxaliplatin
TME	Tumor microenvironment
FAM111B	Family with sequence similarity 111 member B
FANCD2	Fanconi anemia complementation group D2
TMA	Tumor tissue microarray
TCGA	The cancer genome atlas
GTEx	Genotype-tissue expression
GEO	Gene expression omnibus
ROC	Receiver operating characteristic
GO	Gene-ontology
KEGG	Kyoto encyclopedia of genes and genomes
GDSC	Genomics of drug sensitivity in cancer
IC50	Half-maximal inhibitory concentration
ROS	Reactive oxygen species
DPCs	DNA-protein cross-links
LUAD	Lung adenocarcinoma
GBM	Glioblastoma multiforme
PDAC	Pancreatic ductal adenocarcinoma

Supplementary Information

The online version contains supplementary material available at https://doi.org/10.1186/s12935-025-03819-6.

Supplementary Material 1: S.Fig. 1 The clinical significance of FAM111B and FANCD2 expression in a cohort of 78 PDAC cases, excluding 2 cases of adeno-squamous carcinoma, 1 case of ampullary adenocarcinoma (pancreaticobiliary type), 1 case of high-grade intraductal papillary mucinous neoplasm with pancreatic ductal adenocarcinoma, and 1 case of adenocarcinoma. A-D The figure presents the correlations between FAM111B and FANCD2. F-J The survival curves of FAM111B. K-O The survival curves of FANCD2. All figures are depicted across five dimensions: area, cell count, density, H score, and ratio.

Supplementary Material 2: S.Fig. 2 The survival analysis of patients subjected to whether they received adjuvant therapy. A distribution of patients according to whether they received adjuvant therapy. B The survival curves for each group, stratified by the receipt of adjuvant therapy.

Supplementary Material 3: S.Fig. 3 The survival analysis excluding adjuvant therapy cases based on FAM111B and FANCD2 expression. Survival curves for FAM111B (A-E) and FANCD2 (F-J)after excluding adjuvant therapy cases, analyzed in five dimensions: area, cell count, density, H score, and ratio.

Supplementary Material 4: S.Fig. 4 The correlation between FAM111B, FANCD2 and KRAS, TP53 in 78 PDAC patients. A-E The correlation between FAM111B and KRAS. F-J The correlation between FAM111B and TP53. K-O The correlation between FANCD2 and KRAS. P-T The correlation between FAM111B and TP53. All figures are depicted across five dimensions: area, cell count, density, H score, and ratio.

Supplementary Material 5

Acknowledgements
Not applicable.

Author contributions
FW and WYL performed the experiments, drafted the manuscript and analyzed the data. TZ, LJF and XLY analyzed the data from public database and performed the statistics. FW and LHZ were involved in the study conception and design. LHZ supervised the study, reviewed and revised the manuscript. All authors read and approved the final manuscript.

Funding
This work was financially supported by the National Natural Science Foundation of China (Grant No. 81803009), Natural Science Foundation of Hubei Province (Grant No. 2024AFB995), Chinese Society of Clinical Oncology research found (Grant No. Y-L2018-003, Y-sy2018-039), CSCO-BMS Immune-Oncology Research Fund (Grant No. Y-BMS 2019-011), and Chen Xiaoping Foundation for the development of science and technology of Hubei province (Grant No. CXPJJH122006-1027).

Data availability
No datasets were generated or analysed during the current study.

Declarations

Ethics approval and consent to participate
Use of the TMA samples was approved by the Ethics Committee of Shanghai Outdo Biotech Co. Ltd (No. YBM-05-02).Informed consent was signed by each participant.

Consent for publication
Not applicable.

Competing interests
The authors declare no competing interests.

Received: 10 December 2024 / Accepted: 8 May 2025
Published online: 22 May 2025

References

1. Siegel RL, Giaquinto AN, Jemal A, Cancer statistics. 2024. CA Cancer J Clin 2024;74(1):12–49.
2. Park W, Chawla A, O'Reilly EM. Pancreat Cancer: Rev Jama. 2021;326(9):851–62.
3. Di Federico A, Mosca M, Pagani R, Carloni R, Frega G, De Giglio A, Rizzo A, Ricci D, Tavolari S, Di Marco M et al. Immunotherapy in pancreatic cancer: why do we keep failing? A focus on tumor immune microenvironment, predictive biomarkers and treatment outcomes. Cancers (Basel). 2022;14(10).
4. Di Federico A, Tateo V, Parisi C, Formica F, Carloni R, Frega G, Rizzo A, Ricci D, Di Marco M, Palloni A et al. Hacking pancreatic cancer: present and future of personalized medicine. Pharmaceuticals (Basel). 2021;14(7).
5. Turpin A, El Amrani M, Bachet JB, Pietrasz D, Schwarz L, Hammel P. Adjuvant Pancreatic Cancer Management: Towards New Perspectives in 2021; Cancers (Basel). 2020;12(12).
6. Huang L, Jansen L, Balavarca Y, Molina-Montes E, Babaei M, van der Geest L, Lemmens V, Van Eycken L, De Schutter H, Johannesen TB, et al. Resection of pancreatic cancer in Europe and USA: an international large-scale study highlighting large variations. Gut. 2019;68(1):130–9.
7. Neoptolemos JP, Palmer DH, Ghaneh P, Psarelli EE, Valle JW, Halloran CM, Faluyi O, O'Reilly DA, Cunningham D, Wadsley J, et al. Comparison of adjuvant gemcitabine and capecitabine with gemcitabine monotherapy in patients with resected pancreatic cancer (ESPAC-4): a multicentre, open-label, randomised, phase 3 trial. Lancet. 2017;389(10073):1011–24.
8. Tempero MA, Pelzer U, O'Reilly EM, Winter J, Oh DY, Li CP, Tortora G, Chang HM, Lopez CD, Bekaii-Saab T, et al. Adjuvant nab-Paclitaxel + Gemcitabine in resected pancreatic ductal adenocarcinoma: results from a randomized, Open-Label, phase III trial. J Clin Oncol. 2023;41(11):2007–19.
9. Conroy T, Hammel P, Hebbar M, Ben Abdelghani M, Wei AC, Raoul JL, Choné L, Francois E, Artru P, Biagi JJ, et al. FOLFIRINOX or gemcitabine as adjuvant therapy for pancreatic Cancer. N Engl J Med. 2018;379(25):2395–406.
10. Rizzo A, Santoni M, Mollica V, Logullo F, Rosellini M, Marchetti A, Faloppi L, Battelli N, Massari F. Peripheral neuropathy and headache in cancer patients treated with immunotherapy and immuno-oncology combinations: the MOUSEION-02 study. Expert Opin Drug Metab Toxicol. 2021;17(12):1455–66.
11. Guven DC, Erul E, Kaygusuz Y, Akagunduz B, Kilickap S, De Luca R, Rizzo A. Immune checkpoint inhibitor-related hearing loss: a systematic review and analysis of individual patient data. Support Care Cancer. 2023;31(12):624.

12. Sahin TK, Ayasun R, Rizzo A, Guven DC. Prognostic value of Neutrophil-to-Eosinophil ratio (NER) in cancer: A systematic review and Meta-Analysis. Cancers. 2024;16(21).
13. Integrated Genomic Characterization of Pancreatic Ductal Adenocarcinoma. Cancer Cell. 2017;32(2):185–e203113.
14. Kawasaki K, Nojima S, Hijiki S, Tahara S, Ohshima K, Matsui T, Hori Y, Kurashige M, Umeda D, Kiyokawa H, et al. FAM111B enhances proliferation of KRAS-driven lung adenocarcinoma by degrading p16. Cancer Sci. 2020;111(7):2635–46.
15. Li W, Hu S, Han Z, Jiang X. YY1-Induced transcriptional activation of FAM111B contributes to the malignancy of breast Cancer. Clin Breast Cancer. 2022;22(4):e417–25.
16. Wei F, Yu G, Si C, Chao T, Xiong H, Zhang L. High FAM111B expression predicts aggressive clinicopathologic features and poor prognosis in ovarian cancer. Transl Oncol. 2023;32:101659.
17. Gong Q, Dong Q, Zhong B, Zhang T, Cao D, Zhang Y, Ma D, Cai X, Li Z. Clinicopathological features, prognostic significance, and associated tumor cell functions of family with sequence similarity 111 member B in pancreatic adenocarcinoma. J Clin Lab Anal. 2022;36(12):e24784.
18. Mani C, Tripathi K, Chaudhary S, Somasagara RR, Rocconi RP, Crasto C, Reedy M, Athar M, Palle K. Hedgehog/GLI1 transcriptionally regulates FANCD2 in ovarian tumor cells: its Inhibition induces HR-Deficiency and synergistic lethality with PARP Inhibition. Neoplasia. 2021;23(9):1002–15.
19. Miao H, Ren Q, Li H, Zeng M, Chen D, Xu C, Chen Y, Wen Z. Comprehensive analysis of the autophagy-dependent ferroptosis-related gene FANCD2 in lung adenocarcinoma. BMC Cancer. 2022;22(1):225.
20. Tang X, Luo B, Huang S, Jiang J, Chen Y, Ren W, Shi X, Zhang W, Shi L, Zhong X, et al. FANCD2 as a novel prognostic biomarker correlated with immune and drug therapy in hepatitis B-related hepatocellular carcinoma. Eur J Med Res. 2023;28(1):419.
21. Shi Y, Wang Y, Dong H, Niu K, Zhang W, Feng K, Yang R, Zhang Y. Crosstalk of ferroptosis regulators and tumor immunity in pancreatic adenocarcinoma: novel perspective to mRNA vaccines and personalized immunotherapy. Apoptosis. 2023;28(9–10):1423–35.
22. Karim SAM, Abdulla KS, Abdulkarim QH, Rahim FH. The outcomes and complications of pancreaticoduodenectomy (Whipple procedure): cross sectional study. Int J Surg. 2018;52:383–7.
23. Liu Z, Zhao Q, Zuo ZX, Yuan SQ, Yu K, Zhang Q, Zhang X, Sheng H, Ju HQ, Cheng H, et al. Systematic analysis of the aberrances and functional implications of ferroptosis in Cancer. iScience. 2020;23(7):101302.
24. Lian H, Han YP, Zhang YC, Zhao Y, Yan S, Li QF, Wang BC, Wang JJ, Meng W, Yang J, et al. Integrative analysis of gene expression and DNA methylation through one-class logistic regression machine learning identifies stemness features in Medulloblastoma. Mol Oncol. 2019;13(10):2227–45.
25. Kim J, Zhu Y, Chen S, Wang D, Zhang S, Xia J, Li S, Qiu Q, Lee H, Wang J. Anti-glioma effect of ginseng-derived exosomes-like nanoparticles by active blood-brain-barrier penetration and tumor microenvironment modulation. J Nanobiotechnol. 2023;21(1):253.
26. Welter AL, Machida YJ. Functions and evolution of FAM111 Serine proteases. Front Mol Biosci. 2022;9:1081166.
27. Xie X, Zhao Y, Du F, Cai B, Fang Z, Liu Y, Sang Y, Ma C, Liu Z, Yu X, et al. Pan-cancer analysis of the tumorigenic role of Fanconi anemia complementation group D2 (FANCD2) in human tumors. Genomics. 2024;116(1):110762.
28. Dixon SJ, Lemberg KM, Lamprecht MR, Skouta R, Zaitsev EM, Gleason CE, Patel DN, Bauer AJ, Cantley AM, Yang WS, et al. Ferroptosis: an iron-dependent form of nonapoptotic cell death. Cell. 2012;149(5):1060–72.
29. Rochette L, Dogon G, Rigal E, Zeller M, Cottin Y, Vergely C. Lipid peroxidation and Iron metabolism: two corner stones in the homeostasis control of ferroptosis. Int J Mol Sci. 2022;24(1).
30. Friedmann Angeli JP, Krysko DV, Conrad M. Ferroptosis at the crossroads of cancer-acquired drug resistance and immune evasion. Nat Rev Cancer. 2019;19(7):405–14.
31. Hoffmann S, Pentakota S, Mund A, Haahr P, Coscia F, Gallo M, Mann M, Taylor NM, Mailand N. FAM111 protease activity undermines cellular fitness and is amplified by gain-of-function mutations in human disease. EMBO Rep. 2020;21(10):e50662.
32. Li F, He HY, Fan ZH, Li CM, Gong Y, Wang XJ, Xiong HJ, Xie CM, Bie P. Silencing of FAM111B inhibited proliferation, migration and invasion of hepatoma cells through activating p53 pathway. Dig Liver Dis. 2023;55(12):1679–89.
33. Sun H, Liu K, Huang J, Sun Q, Shao C, Luo J, Xu L, Shen Y, Ren B. FAM111B, a direct target of p53, promotes the malignant process of lung adenocarcinoma. Onco Targets Ther. 2019;12:2829–42.
34. Xia P, Sun Y, Zheng C, Hou T, Kang M, Yang X. p53 mediated apoptosis in osteosarcoma MG-63 cells by Inhibition of FANCD2 gene expression. Int J Clin Exp Med. 2015;8(7):11101–8.
35. Liu T, Zhu C, Chen X, Guan G, Zou C, Shen S, Wu J, Wang Y, Lin Z, Chen L, et al. Ferroptosis, as the most enriched programmed cell death process in glioma, induces immunosuppression and immunotherapy resistance. Neuro Oncol. 2022;24(7):1113–25.
36. Li X, Liu J. FANCD2 inhibits ferroptosis by regulating the JAK2/STAT3 pathway in osteosarcoma. BMC Cancer. 2023;23(1):179.
37. Sun X, Ou Z, Chen R, Niu X, Chen D, Kang R, Tang D. Activation of the p62-Keap1-NRF2 pathway protects against ferroptosis in hepatocellular carcinoma cells. Hepatology. 2016;63(1):173–84.

Publisher's note

Springer Nature remains neutral with regard to jurisdictional claims in published maps and institutional affiliations.